BRAF gene status and the expression of growth factor signaling molecules in oral epithelial precursor lesions and squamous cell carcinoma

博 士 論 文

【*BRAF* gene status and the expression of growth factor signaling molecules in oral epithelial precursor lesions and squamous cell carcinoma】

（口腔癌および前駆病変における BRAF 遺伝子の変異と増殖因子シグナル伝達分子の発現に関する研究）

田代　和樹

平成三十年度提出

東北大学

ABSTRACT

Objectives: We analyzed MAPK, Akt, and STAT3 pathway expression and *BRAF* gene status in oral epithelial precursor lesions (OEPLs) and oral squamous cell carcinoma (OSCC).

Study design: Fifteen leukoplakia (LP), 15 low-grade epithelial dysplasia (LD), 15 high-grade epithelial dysplasia (HD), and 132 OSCC specimens were immunohistochemically examined for KRAS, HRAS, NRAS, BRAF, BRAF-V600E, pERK1/2, pAkt, pmTOR, and pSTAT3 expression. *BRAF* mutations were detected by high resolution melting (HRM) analysis, DNA sequencing, and immunohistochemistry.

Results: Immunoreactivity for these molecules predominantly occurred in regions OEPL basal to prickle layers and in most OSCC cells. KRAS and NRAS expression was lower in OSCC than in OEPLs, whereas BRAF-V600E incidence was higher in OSCC than in OEPLs. pERK1/2 expression was higher in HD than in LP. pAkt and pmTOR expression was lower in LP than in other lesions. Correlations between these markers and clinicopathological variables were also noted. Based on HRM, *BRAF* mutations were suspected in seven OEPLs and 34 OSCCs; subsequent DNA sequencing confirmed mutations in one LD, one HD, and five OSCC specimens, which were associated with BRAF-V600E immunoreactivity.

Conclusion: MAPK, Akt, and STAT3 pathways might play diverse roles in oral carcinogenesis. *BRAF* mutations are relatively rare but important aberrations for OSCC.

INTRODUCTION

Oral squamous cell carcinoma (OSCC) comprises a subset of head and neck squamous cell carcinoma (HNSCC) that involves the tongue, gingiva, buccal mucosa, floor of the mouth, and hard palate. OSCC is considered to be the sixth most common oral cancer worldwide.[1,2] Despite improvements in treatment strategies over the past few decades, including surgery and radiotherapy, with or without chemotherapy, the 5-year survival rates (approximately 50%) remain lower than those of most major cancers.[3,4] SCC can be superficial as well as deep, destroying oral cavity tissues and metastasizing to regional lymph nodes or distant organs, most frequently the lung.[5]

Among the oral potentially malignant disorders, leukoplakia is the most commonly encountered lesion and can show histological evidence of hyperkeratosis/squamous cell hyperplasia with or without epithelial dysplasia. Epithelial dysplasia is classified according to the World Health Organization (WHO) classification of tumors of the oral cavity and mobile tongue as follows: low-grade and high-grade based on the presence and severity of cell atypia and structural aspects of the epithelium. Histopathological evaluation of the grade of epithelial dysplasia is the most common method used to ascertain malignant potential in individuals with oral epithelial precursor lesions (OEPLs). Further, the frequency of carcinomatous changes in these oral epithelial precursor lesions has been reported to vary from 6.6% to 36%.[2,6,7]

Several growth factors and their receptors, such as epidermal growth factor receptor (EGFR), have been studied as prognostic biomarkers for many epithelial malignancies. Overexpression of EGFR is associated with poor prognosis in patients with HNSCC.[8,9] Moreover, the downstream signaling pathways affected by activation of these growth factors and their receptors include RAS/RAF/ERK, PI3K/Akt/mTOR, and STAT3.[8,10,11]

The MAPK pathway is a very important signaling pathway for cell proliferation, migration, and survival. RAS GTPase are monomeric G proteins with a molecular mass of 21 kDa that cycle between GTP-bound active and GDP-bound inactive states. The RAS subfamily consists of KRAS, HRAS, and NRAS.[12,13] Activation of RAS initiates a multi-step phosphorylation cascade that leads to the activation of RAF kinase. The RAF subfamily consists of three highly conserved serine/threonine kinases, namely ARAF, BRAF, and CRAF.[14] Among these, the genes encoding B and C isoforms, and especially *BRAF*, were shown to be associated with mutations in cancer.[15] Mutations of *BRAF* have been described in some types of cancers, especially malignant melanoma, papillary thyroid cancer, and colorectal cancer.[15,16] More than 90% of *BRAF* mutations consist of a glutamic acid to valine substitution at amino acid position 600, referred as *BRAF* c.1799 T>A (BRAF-V600E). This substitution leads to constitutive activation of the encoded protein.[17] Activated RAFs phosphorylate the MEK kinase, which finally activates extracellular ERK1/2.[18] The latter signaling molecule is activated by phosphorylation at both tyrosine and threonine residues. Phosphorylated ERK1/2 (pERK1/2) subsequently translocates to the nucleus

and regulates transcriptional programs related to cell proliferation.[19] In HNSCC, levels of pERK1/2 expression were found to correlate with increased nodal metastasis, proliferative rate, and recurrence.[8]

The PI3K/Akt/mTOR pathway also plays a fundamental role in tumorigenesis.[9] This signaling cascade begins with PI3K activation at the cell membrane, followed by Akt activation. Akt is a serine/threonine protein kinase that requires phosphorylation for activation. Phosphorylated Akt (pAkt) regulates the activity of numerous downstream molecules including mTOR, which has emerged as an essential effector of cell signaling pathways.[20,21] mTOR is also a serine/threonine protein kinase that requires phosphorylation for activation. pAkt and phosphorylated mTOR (pmTOR) translocate from the cytoplasm to the nucleus leading to the transcription of genes responsible for cell cycle progression and cellular proliferation.[21,22]

STAT3 is a member of the STAT family, which participates in many physiological processes, such as cell proliferation, survival, and differentiation.[23] Constitutive activation of STAT3 has been demonstrated in several human cancers including lung cancer, breast cancer, colon cancer, and HNSCC.[10,23] STAT3 tyrosine phosphorylation can be induced by stimulation via upstream receptor and/or nonreceptor kinases including EGFR, IL-6, JAK, and Src. Phosphorylated STAT3 (pSTAT3) dimerizes and translocates to the nucleus to regulate the transcription of the target genes.[24] Recent studies have shown that the expression of pSTAT3 is associated with lymph node metastasis, recurrence, and poor prognosis in HNSCC.[24,25]

The present study was designed to assess the role of MAPK, Akt, and

STAT3 pathways in OSCC and OEPLs. In addition, mutations of the *BRAF* gene and BRAF-V600E protein expression were analyzed in these specimens.

MATERIALS AND METHODS

The study protocol was reviewed and approved by the Research Ethics Committee of Tohoku University Graduate School of Dentistry (2017-3-2).

Clinicopathological characteristics

Specimens were surgically removed from 132 patients with primary OSCC and 45 patients with OEPLs in the Department of Oral and Maxillofacial Surgery, Tohoku University Hospital from 2012 through 2016. All OSCC patients had never received chemotherapy or radiotherapy before surgery. The TNM disease stage was classified according to the Union for International Cancer Control (UICC) system.[26] None of the OEPLs patients were diagnosed as OSCC at any of the sites before surgery or progressed to OSCC.

Sample preparation

Tissue samples were fixed in 10% buffered formalin for several days and embedded in paraffin. The tissue blocks were sliced into 4-μm-thick sections for routine histological examination and subsequent immunohistochemical and genetic analyses. The tumor histological grade was determined according to the World Health Organization classification.[2] The mode of tumor invasion was classified as previously described [27]; carcinoma grade was 2, 3, 4C, and 4D. The invasion depth was classified into microinvasion and invasion within the mucosal tissue and into the submucosal tissue. Lymphoplasmacytic infiltration was determined on hematoxylin and eosin stained specimens according to the Anneroth classificassion.[2]

OEPLs pathological diagnoses were made according to the WHO classification of tumors of the oral cavity and mobile tongue.[2] In all, fifteen patients had leukoplakia without epithelial dysplasia (hyperkeratosis or squamous cell hyperplasia; LP), 15 had low-grade epithelial dysplasia (mild to moderate dysplasia; LD), and 15 had high-grade epithelial dysplasia (severe dysplasia or carcinoma in situ; HD).

Immunohistochemistry for KRAS, HRAS, NRAS, BRAF, BRAF-V600E, pERK1/2, pAkt, pmTOR, and pSTAT3 expression

Tissue sections were deparaffinized and immersed in methanol with 0.3% hydrogen peroxide. The sections were heated in 0.01 M citrate buffer (pH 6.0; for HRAS and NRAS) or 1 mM ethylenediamine tetraacetic acid (EDTA) buffer (pH 9.0; for BRAF, BRAF-V600E, pERK1/2, pAkt, pmTOR, and pSTAT3) for 10 min by autoclaving (121 °C, 2 atm). Specimens were then incubated with primary antibodies at 4 °C overnight. The applied antibodies were mouse anti-KRAS monoclonal (ProteinTech, Chicago, IL, USA; isotype IgG1, diluted at 1:100), rabbit anti-HRAS polyclonal (ProteinTech; isotype IgG, diluted at 1:50), rabbit anti-NRAS polyclonal (ProteinTech; isotype IgG, diluted at 1:50), rabbit anti-BRAF monoclonal (Abcam, Cambridge, UK; isotype IgG, diluted at 1:250), mouse anti-BRAF-V600E monoclonal (Spring Bioscience, Pleasanton, CA, USA; isotype IgG2a, diluted at 1:100), rabbit anti-ERK1 (phospho Thr202 + Tyr204) / ERK2 (phospho Thr185 + Tyr187) monoclonal (Abcam; isotype IgG1, diluted at 1:100), rabbit anti-phospho-Akt1/2/3 (Thr308) polyclonal (Santa Cruz, Dallas, TX, USA; isotype IgG, diluted at 1:100), rabbit anti-phospho-mTOR (Ser2448) polyclonal (Signalway Antibody, Pearland, TX, USA; isotype IgG, diluted at 1:100), and rabbit anti- phospho-STAT3 (Tyr705) monoclonal (Abcam; isotype IgG, diluted at 1:100). The sections were then incubated with peroxidase-conjugated anti-mouse IgG (for KRAS and BRAF-V600E) or anti-rabbit IgG (for HRAS, NRAS, BRAF, pERK1/2, pAkt, pmTOR, and pSTAT3) polyclonal antibodies (Histofine Simple Stain MAX-PO; Nichirei,

Tokyo, Japan) for 45 min, and reaction products were visualized by immersing the sections in 0.03% diaminobenzidine (DAB) solution containing 2 mM hydrogen peroxide for 3 to 5 min. Nuclei were lightly stained with Mayer's hematoxylin. Slides for pERK1/2 were also exposed using the streptavidin–biotin method (Histofine SAB-PO kit; Nichirei). For antibody negative control experiments, the serial sections were treated with phosphate-buffered saline (PBS), normal rabbit IgG, mouse anti-OPD4 (CD45RO) monoclonal antibody (Dako, Glostrup, Denmark; isotype IgG1), and mouse anti-alpha-smooth muscle actin monoclonal antibody (Dako; isotype IgG2a) instead of primary antibodies and were confirmed to be unstained.

Evaluation of immunohistochemical results

Immunohistochemical reactivity for KRAS, HRAS, NRAS, BRAF, pERK1/2, pAkt, pmTOR, and pSTAT3 was evaluated and classified into two groups as follows: (+) positive (reactive at the same level as adjacent normal part) and (++) strongly positive (strongly reactive as compared to staining in the adjacent normal part). BRAF-V600E antibody staining was scored as (+) positive when the tumor cells showed clear cytoplasmic staining, and (–) negative when there was no staining or only nuclear dot staining. Cases were scored as (±) weak positive or ambiguous if immunostaining could not be evaluated as positive or negative.

DNA extraction

DNA was extracted from 10-μm-thick sections of paraffin-embedded tumor tissue blocks in 80 μL of elution buffer using the MagNa Pure LC DNA Isolation Kit II (Roche, Mannheim, Germany), after deparaffinization with xylene and overnight proteinase K digestion.

High resolution melting (HRM) analysis

BRAF mutations were detected by HRM analysis followed by pyrosequencing on a LightCycler® 480 Instrument (Roche). HRM analysis was performed using 1 μL of genomic DNA, 2 μL of 2.5 mM $MgCl_2$, 10 μL of Master Mix, 0.4 μL of primer (10 μM each), and 6.2 μL of dH_2O in a final reaction volume of 20 μL. Thermocycling conditions for PCR included one cycle denaturation at 95 °C for 10 min and 50 cycles consisting of denaturation at 95°C for 20 s, annealing at 55 °C for 20 s, and extension at 72 °C for 15 s, with subsequent cooling at 40 °C for 30 s. Primer sequences were as follows: forward 5′- CATAATGCTTGCTCTCTGATAGGAAA -3′ and reverse 5′- TCAGCACACATCTCAGGGCCAAA -3′. HRM curve analysis was performed using LightCycler® 480 Gene Scanning Software Version 1.5 (Roche). Normalized and temperature-adjusted melting curves of test samples and wild type controls were compared, and samples with an aberrant melting pattern were judged to harbor a somatic mutation.

Direct DNA sequencing for *BRAF* gene mutations

Amplified products of mutation-positive or ambiguous samples, as detected by HRM analysis, were recovered from the plate and purified with the Wizard® SV Gel and PCR Clean-up System (Promega, Madison, WI, USA); direct DNA sequencing was performed using an ABI Prism 3100 Genetic Analyzer (Applied Biosytems, Carlsbad, CA, USA).

Statistical analysis

The statistical significance of differences in immunohistochemical reactivity, HRM analysis, DNA sequencing, and correlation analyses were tested by the Mann–Whitney *U*-test for differences between two groups or the Kruskal–Wallis test for differences among three or more groups. *P* values less than 0.05 were considered to indicate statistical significance.

RESULTS

Patient characteristics

Details of patient characteristics were shown in Table 1. Ages ranged from 25 to 95 years (mean, 66.8 years); 70 were men and 62 were women. Seventy-one carcinomas were located in the tongue, 11 in the upper gingiva, 24 in the lower gingiva, two in the hard palate, 11 in the buccal mucosa, 10 in the floor of the mouth, and three in the lower lip, respectively. The T

classifications were T1 for 40 cases, T2 for 41, T3 for 17, and T4 for 34, the N classifications were N0 for 100 cases, N1 for nine, N2 for 22, and N3 for one; M classifications were M0 for 126 cases and M1 for six cases. According to overall TNM stage grouping, 36 patients had stage I, 38 had stage II, 20 had stage III, and 38 had stage IV disease. During the follow-up period (23–66 months), local recurrence occurred in 19 patients and post-operative regional lymph node metastasis was noted in 16 patients. Nineteen patients died of OSCC and two died of unrelated causes. The histological grade was well-differentiated in 110 of the patients, moderately -differentiated in 18 of the patients, and poorly-differentiated in 4 of the patients. The degree of stromal lymphocytic reaction was classified as slight for 12 specimens, moderate for 118, and severe for two. The mode of tumor invasion grade was 2 for 17 specimens, 3 for 85, 4C for 24, and 4D for 6. The invasion depth was microinvasion for 36, invasion within the mucosal tissue for 51, and the submucosal tissue for 45 tumors, respectively.

Immunohistochemical reactivity of KRAS, HRAS, NRAS, BRAF, BRAF-V600E, pERK1/2, pAkt, pmTOR, and pSTAT3 in OEPLs and OSCC

The results of immunohistochemical studies of KRAS, HRAS, NRAS, BRAF, BRAF-V600E, pERK1/2, pAkt, pmTOR, and pSTAT3 expression in OEPLs and OSCC are summarized in Table I and Figures1–3.

KRAS immunohistochemical reactivity was detected in the cytoplasm, with occasional membrane localization in epithelial cells of OEPLs (Figure 1F, 1G, and 1H), and in the cytoplasm of most OSCC cells (Figure 1I and 1J). KRAS immunohistochemical reactivity was significantly decreased in OSCC compared to that in LP ($P < .001$), LD ($P < .001$), and HD ($P < .001$) (Table I). HRAS and NRAS immunoreactivity were detected in the cytoplasm of epithelial cells of OEPLs and OSCC (Figure 1K–1O, 1P–1T). HRAS and NRAS reactivity was detected in the basal and parabasal cell layer of OEPLs (Figure 1K–1M, 1P–1R) and in most OSCC cells (Figure 1N, 1O, 1S, and 1T). NRAS immunohistochemical reactivity was significantly decreased in OSCC compared to thay in LP ($P < .001$), LD ($P < .001$), and HD ($P < .001$) (Table I).

Moderate to strong cytoplasmic BRAF staining was observed in basal cell and prickle cell layers of OEPLs (Figure 2F–2H) and in most OSCC cells (Figure 2I and 2J). Weak cytoplasmic BRAF-V600E reactivity was observed in basal to prickle cell layers of one LD and one HD case. For OSCC specimens, weak cytoplasmic staining was noted in most carcinoma cells in 29 cases and moderate to strong cytoplasmic staining was observed in most carcinoma cells in five cases. Immunohistochemical reactivity for BRAF-V600E was significantly increased in OSCC compared to that in LP (P

< .05; Table I). pERK1/2 immunoreactivity was detected in the cytoplasm and nuclei of epithelial cells of OEPLs and OSCC. pERK1/2 reactivity was detected in basal and parabasal cell layers of OEPLs (Figure 2P–2R) and in most OSCC cells (Figure 2S and 2T). Immunohistochemical reactivity for pERK1/2 was significantly enhanced in HD compared to that in LP (P< .05; Table I).

pAkt and pmTOR immunoreactivity was detected in the cytoplasm and nuclei of epithelial cells of OEPLs and OSCC (Figure 3F–3J, 3K–3O). pAkt and pmTOR reactivity, with co-localization, was detected in basal and prickle cell layers of OEPLs (Figure 3K–3M, 3P–3R). OSCC exhibited pAkt and pmTOR reactivity in most carcinoma cells (Figure 3N, 3O, 3S, 3T). Immunohistochemical reactivity for pAkt was significantly enhanced in OSCC compared to that in LP (P< .01; Table I). Further, pmTOR reactivity was significantly decreased in LP compared to that in LD (P< .001), HD (P < .001), and OSCC (P< .001) (Table I). pSTAT3 immunoreactivity was detected in the cytoplasm and nuclei of epithelial cells of OEPLs and OSCC (Figure 3P–3T). pSTAT3 reactivity was detected in basal and prickle cell layers of OEPLs (Figure 2P–2R) and OSCC exhibited pSTAT3 reactivity in most carcinoma cells (Figure 3S and 3T).

Correlation between clinicopathological variables and KRAS, HRAS, NRAS, BRAF, BRAF-V600E, pERK1/2, pAkt, pmTOR, and pSTAT3 immunoreactivity in OSCC

KRAS, HRAS, NRAS, BRAF, BRAF-V600E, pERK1/2, pAkt, pmTOR, and

pSTAT3 immunohistochemical reactivities in 132 OSCC specimens were compared to underlying clinicopathological variables (Table II and III).

The expression of KRAS in tumors was higher in patients with the following clinicopathological characteristics: patients in their 80s rather than patients in their 40s ($P < .001$), 60s ($P < .001$), and 70s ($P < .001$); and males rather than females ($P < .001$) (Table II). A weak correlation between KRAS expression and M classification was also found without reaching statistical significance ($P = .060$). KRAS expression was also associated with tumor site based on an analysis of variance ($P < .05$), but significant differences were not noted based on multivariate analysis (Table II). No clinicopathological variables were found to correlate with HRAS expression. The expression of NRAS in tumors was higher in patients with the following clinicopathological characteristics: patients in their 80s rather than patients in their 50s ($P < .001$), 60s ($P < .001$), and 70s ($P < .01$); males rather than females ($P < .001$); tongue rather than lower gingiva ($P < .05$) (Table II).

A weak correlation between BRAF expression and sex was also found without reaching statistical significance ($P = .067$; Table II). Further, the expression of BRAF-V600E was higher in cases with post-operative metastasis ($P < .05$) (Table II). In addition, the expression of pERK1/2 was higher in tumors with the following clinicopathological characteristics: female patients ($P < .05$); T4 cases rather than T2 cases ($P < .01$), and TNM stage IV cases rather than TNM stage II cases ($P < .01$) (Table II).

The expression of pAkt was higher in T4 cases than in T2 cases ($P < .05$) and in cases without post-operative metastasis (as compared to those with

metastasis; $P < .05$) (Table II). Moreover, the expression of pmTOR was higher in grade 2 and 4C mode of invasion cases, as compared to that in grade 4D cases ($P < .05$; Table III). In addition, the expression of pSTAT3 was decreased in tumors with the following clinicopathological characteristics: cases without recurrence (as compared to those with recurrence; $P < .05$); hard palate rather than tongue ($P < .01$), upper gingiva ($P < .05$), lower gingiva ($P < .01$), buccal mucosa ($P < .01$), and lower lip ($P < .05$) (Table II); cases of microinvasion rather than those with mucosal ($P < .05$) and submucosal invasion ($P < .05$) (Table III).

Identification of *BRAF* mutations using HRM, direct DNA sequencing, and IHC in OEPLs and OSCC

The results of IHC assays, HRM analysis, and direct sequencing of *BRAF* mutations are shown in Table IV and Figure 4. A total of 177 patients were analyzed for *BRAF* mutations by both HRM analysis and IHC assays, including 132 cases of OSCC, 15 cases of LP, 15 cases of LD, and 15 cases of HD. Among the 177 cases, IHC staining was positive in 36 cases including one case (of 15, 6.7%) of LD, one case (of 15, 6.7%) of HD, and 34 cases (of 132, 25.8%) of OSCC (Figure 4E, 4J). Forty-one cases were recorded as HRM-positive or ambiguous, including four cases (of 15, 26.7%) of LP, two cases (of 15, 13.3%) of LD, one case (of 15, 6.7%) of HD, and 34 cases (of 132, 25.8%) of OSCC (Figure 4A, 4B, 4F, 4G). A total of 41 positive or ambiguous cases, based on HRM, were subjected to sequencing to confirm the mutation. Seven mutation-positive cases were confirmed by direct sequencing,

including one case of LD, one case of HD, and five cases of OSCC (Figure 4C, 4D, 4H, 4I).

Correlations between DNA sequencing and IHC to detect *BRAF* mutations

The results of correlation analysis comparing IHC and molecular data are presented in Table V. All seven *BRAF* mutation-positive cases detected by direct DNA sequencing were also positive based on IHC, including two cases of OEPLs (weak positive) and five cases in OSCC (strong positive) (Table V). The correlations between IHC reactivity and DNA sequencing were significant for both OEPLs ($P < .05$) and OSCC ($P < .001$) (Table V). Further, the clinicopathological features of seven *BRAF*-mutated cases are presented in Table VI.

DISCUSSION

The oncogenic role of aberrant MAPK, Akt, and STAT3 signaling pathway activation has been investigated in various malignancies including head and neck cancer. The MAPK pathway regulates all critical phases of cell growth including proliferation, differentiation, and apoptosis, and deregulation of this pathway has been reported in several types of tumors.[22]

MAPK pathway

In the present study, significant loss of KRAS and NRAS immunoreactivity was found in OSCC as compared to expression in OEPLs. Vairaktaris et al showed that the NRAS immunoreactivity decreased during the following stages of oncogenesis.[12] In contrast, Jian et al have reported that the expression of RAS was undetectable in precancer lesions but was found in esophageal squamous cell carcinoma.[28] These features suggest that KRAS and NRAS activation might represent a relatively early alteration in oral carcinogenesis. Previous studies have also demonstrated HRAS expression in normal, benign, dysplastic, and malignant lesions for bladder and breast cancer.[29,30] In our study, HRAS expression was constitutively observed in OEPLs and OSCC, suggesting that its activation might have a role in oral carcinogenesis. In our study, BRAF immunoreactivity was found in most OEPLs and OSCC, whereas BRAF-V600E expression was not observed in no dysplastic leukoplakia but was detected in lesions with dysplastic changes, especially in OSCC. These results suggest that wild type BRAF functions in a constitutive manner during oral carcinogenesis and that the mutation of this protein gene might be limited to OSCC development. In the present study, pERK1/2 expression tended to increase in oral lesions with dysplastic changes including OSCC, as compared to that in tissues without dysplastic lesions, and was highest in HD. Chang et al showed that pERK1/2 expression is low in normal cervical tissues, but is significantly higher in cervical intraepithelial neoplasia, when compared to that in cervical carcinoma, at both the transcriptional and translational levels.[31] These

features suggest that pERK1/2 expression could be an early and potentially critical event during oral cancer development.

We found that increased levels of KRAS and NRAS significantly correlate with age, male gender, and disease site. In addition, HRAS and BRAF expression tended to be higher in men than in women. Mahmoud et al also showed that KRAS immunoreactivity in tumor specimens tended to be higher in males than in females with colorectal carcinoma.[13] We also confirmed that HRAS and BRAF immunoreactivity tended to increase with M classification, recurrence, lymph node metastasis, survival, and mode of invasion, suggesting that these markers might be involved in the progression and prognosis of OSCC. Several reports have indicated that *BRAF* mutations are associated with clinicopathological features including female gender, advanced stage, tumor location, lymph node metastasis, recurrence, and poor differentiation in colorectal and thyroid carcinoma.[18,32] Our data showed that BRAF-V600E reactivity tended to be slightly more frequent in males and with early stages of OSCC. We also found a significant association between BRAF-V600E reactivity and postoperative lymph node metastasis, as well as slightly higher BRAF-V600E expression in cases with grade 3, 4C, and 4D modes of invasion. These features suggest that BRAF mutations might be associated with the aggressive behavior of OSCC cells. Several reports have indicated that pERK1/2 is associated with clinicopathological features including cell proliferation, differentiation, survival, invasion, lymph node metastasis, and recurrence in HNSCC.[8,19] Wang et al reported that pERK1/2 expression is associated with T stage,

resulting in advanced TNM stage.[33] In the present study, pERK1/2 expression was higher in females than in males. In addition, we found that the expression of pERK1/2 in OSCC correlates with advanced TNM stage, and especially T classification, and that pERK1/2 expression tends to increase according to recurrence, postoperative lymph node metastasis, and patient death. These features suggest that this marker might be involved in the progression of OSCC. Further, pERK1/2 immunoreactivity tended to be higher with poor differentiation and advanced invasion depth, suggesting that it could be correlated with carcinoma cell differentiation and OSCC prognosis.

BRAF mutations

BRAF mutations result in constitutive activation of the encoded protein and its downstream MAPK pathway, which promotes proliferation and tumorigenesis. The detection of *BRAF* mutations has been reported using several different molecular techniques such as direct DNA sequencing, allele-specific real-time quantitative polymerase chain reaction, pyrosequencing, and HRM. HRM analysis is a recently developed molecular technique proven to be applicable for the detection of various clinically relevant mutations in humans. In addition, the PCR amplification products obtained from HRM analysis can be directly used for direct sequencing without pretreatment.[34] Moreover, IHC using a BRAF-V600E specific antibody has been utilized to detect *BRAF* mutations in various tumors including malignant melanoma, thyroid carcinoma, and pulmonary

carcinoma.[16] It was previously established that the immunohistochemical detection of mutant BRAF-V600E can be used in clinical practice as a first test to screen for *BRAF* mutations.[17] In the present study, we used a combined strategy to screen mutations. All samples were first analyzed by HRM and IHC, and then suspected positive samples were subjected to direct DNA sequencing. We found that 2/45 (4.4%) OEPLs and 34/132 (25.8%) OSCCs were positive for BRAF-V600E by IHC, whereas 7/45 (15.6%) OEPLs and 34/132 (25.8%) OSCCs were positive or ambiguous for *BRAF-V600E* based on HRM. Regarding the detection of *BRAF* mutations, there was no prominent correlation between IHC and HRM. However, we revealed that IHC reactivity significantly correlated with *BRAF* mutations identified by direct DNA sequence. Thus, we confirmed that two weak-positive OEPL cases and five strong-positive OSCC cases, based on IHC, comprised *BRAF* mutant cases. Our results demonstrated that BRAF-V600E IHC could be useful for screening the mutational status of OSCC.

BRAF mutations have been reported in several studies, and the mutation rates have ranged from 0% to 3% for HNSCC samples.[14,15,35] In the present study, *BRAF* mutations were identified in five cases (3.8%) of OSCC samples and two cases (4.4%) of OEPLs samples. These OSCC cases predominantly included early stage disease, but included recurrent, metastatic, poorly differentiated, and grade 4C–D invasion cases. The frequency of mutations in OSCC and OEPLs was similar to that reported in other studies, suggesting that *BRAF* mutations are somewhat rare and that they represent a relatively early alteration in the oral mucosal epithelium.

Akt pathway

Akt signaling is known to be frequently activated in human cancers.[9, 21] In our study, pAkt expression in LP was detected predominantly in the cytoplasm of epithelial cells, whereas pmTOR was detected in the cytoplasm and nuclei. In LD, HD, and OSCC, pAkt and pmTOR were localized to the nuclei and cytoplasm of epithelial or carcinoma cells. Previous studies have shown variable distribution of pAkt in different cellular compartments of oral premalignant and malignant lesions, indicating that pAkt localization might be related to differences in activity.[36,37] It has been reported that active Akt and mTOR localize mainly in the cytoplasm of tumor cells, although the ratio of nuclear to cytoplasmic reactivity was found to increase during tumor progression.[38,39] Recent studies demonstrated that pAkt expression in OSCC is significantly increased when compared to that in the normal epithelium and epithelial dysplasia.[36,37] Balsara et al reported that dysplastic lung tissue contains a high concentration of pAkt, which could further promote the malignant transformation of precancerous cells.[20] Our analysis revealed significantly enhanced pAkt reactivity in OSCC compared to that in LP, and this tended to be lower in HD than in LD. In addition, pmTOR reactivity was significantly decreased in LP compared to that in LD, HD, and OSCC, but there was no apparent relationship among LD, HD, and OSCC, as observed by Martins et al.[21] These features suggest that pAkt and pmTOR expression could contribute to an early and potentially critical event required for the progression from dysplastic lesions to oral cancer.

In this study, increased expression of pAkt was significantly correlated with

advanced T stage and tended to be higher with M stage, differentiation, and invasion depth. In addition, we found that pAkt expression was significantly higher in tumors form patients with negative lymph node metastasis as compared to that in patients with positive lymph node metastasis. These results support previously studies on patients with gastric carcinomas and HNSCC.[9,40] In contrast, Lim et al have indicated pAkt expression correlates with lymph node metastasis and clinical stage, which remains a significant prognostic factor for OSCC.[41] We also confirmed that pAkt tended to increase with low differentiation and deep invasion. Hutchinson et al. reported that pAkt is closely associated with invasion and metastasis.[42] These features suggest that pAkt might correlate with disease stage and could be a prognostic factor. In the present study, pmTOR overexpression was significantly correlated with advanced T stage, lymph node metastasis, and differentiation in OSCC.[21,39] mTOR inhibition has been found to decrease cell migration and invasion depending on the cell system, thus indicating that its activation is correlated with cancer cell invasion and distant metastasis.[43,44] However, previous reports have also indicated that there is no significant correlation between pmTOR expression and any clinical factors for OSCC and lung cancer.[10,22] The present data showed that increased expression of pmTOR was significantly correlated with mode of invasion. These features suggest that mTOR might play a role in the progression and morphologic characteristics of OSCC.

STAT3 pathway

Increasing evidence supports the critical role of STAT3 in malignant transformation and tumor progression.[11,23] Grandis et al. showed that pSTAT3 is detected only in the basal epithelial layer, based on a representative normal mucosal sample from a patient without cancer. In contrast, pSTAT3 is present throughout the entire epithelium in normal mucosal sections from cancer patients and is overexpressed in neoplastic regions.[10] Muzafar et al. demonstrated that increased nuclear accumulation of pSTAT3 occurs during early premalignant stages and assumed that it is a predictor of poor prognosis in OSCC.[4] In our study, OSCC samples showed intermediate nuclear and cytoplasmic pSTAT3 staining in most carcinoma cells as described previously, whereas OEPLs exhibited pSTAT3 reactivity in limited epithelial portions, suggesting that its participates in invasive growth. In the oral mucosa, STAT3 activation might occur as a relatively late event in carcinogenesis and could serves as a biomarker for invasiveness.

Several reports have indicated that activated STAT3 is associated with clinicopathological features, including tumor stage, lymph node metastasis, recurrence, differentiation, and decreased survival in HNSCC.[4,23,24] Neelam et al. revealed that in specimens from early-stage OSCC with nuclear STAT3 immunoreactivity, patients are 3.23-times more likely to develop recurrence when compared to patients with early-stage disease devoid of STAT3 immunoreactivity.[24] In the present study, we found that increased pSTAT3 levels significantly correlate with recurrence and invasion depth, and pSTAT3 reactivity tended to increase according to TNM stage, lymph node

metastasis, survival, differentiation degree, and mode of invasion. Cumulatively, our results suggest that STAT3 contributes to the aggressive behavior of cancers, and is related to poor prognosis in oral mucosal cancer and precancerous lesions; moreover, STAT3 signaling might represent a promising therapeutic target for head and neck cancer.

CONCLUSION

We analyzed the activation of growth factor downstream signaling molecules including MAPK, Akt, and STAT3 in OSCC and OEPLs, and this was compared to relevant clinicopathologic variables in OSCC. In addition, the correlation between *BRAF*-V600E gene mutations and product protein expression was investigated in these precancerous and malignant lesions. This resulted in the delineation of critical pathways involved in carcinogenesis, which could be exploited to direct pharmaceutical intervention.

REFERENCES

1. Warnakulasuriya S. Global epidemiology of oral and oropharyngeal cancer. *Oral Oncol.* 2009; 45: 309-316.
2. El-Naggar AK, Chan JKC, Grandis JR, Takata T, Slootweg PJ. *WHO classification of head and neck tumours*. 4th ed. Lyon, France: IARC Press: 2017; 105-131
3. Gorsky M, Epstein JB, Oakley C, Le ND, Hay J, Stevenson-Moore P. Carcinoma of the tongue: a case series analysis of clinical presentation, risk factors, staging, and outcome. *Oral Surg Oral Med Oral Pathol Oral Radiol Endod*. 2004;98: 546-552.
4. Macha MA, Matta A, Kaur J, et al. Prognostic significance of nuclear pSTAT3 in oral cancer. *Head Neck*. 2011;33:482-489.
5. Woolgar JA. Histopathological prognosticators in oral and oropharyngeal cell carcinoma. *Oral Oncol*. 2006 ;42:229-239.
6. Holmstrup P, Vedtofte P, Reibel J, Stoltze K. Long - term treatment outcome of oral premalignant lesions. *Oral Oncol*. 2006 ;42:461-474.
7. Nguyen CT, Okamura T, Morita KI, et al. LAMC2 is a predictive marker for the malignant progression of leukoplakia. *J Oral Pathol Med*. 2017; 46: 223–231.
8. Albanell J, Codony-Servat J, Rojo F, et al. Activated extracellular signal-regulated kinases: association with epidermal growth factor receptor/transforming growth factor alpha expression in head and neck squamous carcinoma and inhibition by anti-epidermal growth factor

receptor treatments. *Cancer Res*. 2001;61:6500-6510.

9. Nijkamp MM, Hoogsteen IJ, Span PN, et al. Spatial relationship of phosphorylated epidermal growth factor receptor and activated AKT in head and neck squamous cell carcinoma. *Radiother Oncol*. 2011 ;101:165-170.
10. Grandis JR, Drenning SD, Zeng Q, et al. Constitutive activation of Stat3 signaling abrogates apoptosis in squamous cell carcinogenesis in vivo. *Proc Natl Acad Sci U S A*. 2000;97:4227-4232.
11. Won HS, Jung CK, Chun SH, et al. Difference in expression of EGFR, pAkt, and PTEN between oropharyngeal and oral cavity squamous cell carcinoma. *Oral Oncol*. 2012 ;48:985-990.
12. Vairaktaris E, Papageorgiou G, Derka S, et al. Expression of ets-1 is not affected by N-ras or H-ras during oral oncogenesis. *J Cancer Res Clin Oncol*. 2007 ;133:227-233.
13. Elsabah MT, Adel I. Immunohistochemical assay for detection of K-ras protein expression in metastatic colorectal cancer. *J Egypt Natl Canc Inst*. 2013 ;25:51-56.
14. Weber A, Langhanki L, Sommerer F, Markwarth A, Wittekind C, Tannapfel A. Mutations of the BRAF gene in squamous cell carcinoma of the head and neck. *Oncogene*. 2003;22:4757-4759.
15. Davies H, Bignell GR, Cox C, et al. Mutations of the BRAF gene in human cancer. *Nature*. 2002;417:949-954.
16. Na JI, Kim JH, Kim HJ, et al. VE1 immunohistochemical detection of the BRAF V600E mutation in thyroid carcinoma: a review of its usefulness

and limitations. *Virchows Arch*. 2015;467:155-168.

17. Bodnar M, Burduk P, Antosik P, Jarmuz-Szymczak M, Wierzbicka M, Marszalek A, et al. Assessment of BRAF V600E (VE1) protein expression and BRAF gene mutation status in codon 600 in benign and malignant salivary gland neoplasms. *J Oral Pathol Med*. 2017;46:340-345.
18. Liu C, Chen T, Liu Z. Associations between BRAF(V600E) and prognostic factors and poor outcomes in papillary thyroid carcinoma: a meta-analysis. *World J Surg Oncol*. 2016;14:241
19. Pouysségur J, Volmat V, Lenormand P. Fidelity and spatio-temporal control in MAP kinase (ERKs) signalling. *Biochem Pharmacol*. 2002;64:755-763.
20. Balsara BR, Pei J, Mitsuuchi Y, et al. Frequent activation of AKT in non-small cell lung carcinomas and preneoplastic bronchial lesions. *Carcinogenesis*. 2004;25:2053-2059.
21. Martins F, de Sousa SC, Dos Santos E, Woo SB, Gallottini M. PI3K-AKT-mTOR pathway proteins are differently expressed in oral carcinogenesis. *J Oral Pathol Med*. 2016;45:746-752.
22. Pelloski CE, Lin E, Zhang L, et al. Prognostic associations of activated mitogen-activated protein kinase and Akt pathways in glioblastoma. *Clin Cancer Res*. 2006;12:3935-3941.
23. Wang Y, Guo W, Li Z, et al. Role of the EZH2/miR-200 axis in STAT3-mediated OSCC invasion. *Int J Oncol*. 2018;52:1149-1164.
24. Shah NG, Trivedi TI, Tankshali RA, et al. Prognostic significance of molecular markers in oral squamous cell carcinoma: a multivariate

analysis. *Head Neck*. 2009;31:1544-1556.

25. Zhao Y, Zhang J, Xia H, et al. Stat3 is involved in the motility, metastasis and prognosis in lingual squamous cell carcinoma. *Cell Biochem Funct*. 2012;30:340-346.
26. Sobin LH, Gospodarowicz MK, Wittekind C. *TNM Classification of Malignant Tumors*. 5th ed. New York: John Wiley & Sons, Inc.; 2009; 22-29
27. Yamamoto E, Miyakawa A, Kohama G. Mode of invasion and lymph node metastasis in squamous cell carcinoma of the oral cavity. *Head Neck Surg*. 1984;6:938-947.
28. Li J, Feng CW, Zhao ZG, Zhou Q, Wang LD. A preliminary study on ras protein expression in human esophageal cancer and precancerous lesions. *World J Gastroenterol*. 2000;6:278-280.
29. Sardon D, de la Fuente I, Calonge E, et al. H-ras immunohistochemical expression and molecular analysis of urinary bladder lesions in grazing adult cattle exposed to bracken fern. *J Comp Pathol*. 2005;132:195-201.
30. Calaf GM, Abarca-Quinones J. Ras protein expression as a marker for breast cancer. *Oncol Lett*. 2016;11:3637-3642.
31. Chang H, Shi Y, Tuokan T, Chen R, Wang X. Expression of aquaporin 8 and phosphorylation of Erk1/2 in cervical epithelial carcinogenesis: correlation with clinicopathological parameters. Int *J Clin Exp Pathol*. 2014;7:3928-3937.
32. Li Y, Li W. BRAF mutation is associated with poor clinicopathological outcomes in colorectal cancer: A meta-analysis. *Saudi J Gastroenterol*.

2017;23:144-149.

33. Wang JP, Hu WM, Wang KS, et al. Expression of C-X-C chemokine receptor types 1/2 in patients with gastric carcinoma: Clinicopathological correlations and significance. *Oncol Lett*. 2013;5:574-582.
34. Borràs E, Jurado I, Hernan I, et al. Clinical pharmacogenomic testing of KRAS, BRAF and EGFR mutations by high resolution melting analysis and ultra-deep pyrosequencing. BMC Cancer. 2011;11:406.
35. Bruckman KC, Schönleben F, Qiu W, Woo VL, Su GH. Mutational analyses of the BRAF, KRAS, and PIK3CA genes in oral squamous cell carcinoma. *Oral Surg Oral Med Oral Pathol Oral Radiol Endod*. 2010;110:632-637.
36. Pontes HA, de Aquino Xavier FC, da Silva TS, et al. Metallothionein and p-Akt proteins in oral dysplasia and in oral squamous cell carcinoma: an immunohistochemical study. *J Oral Pathol Med*. 2009;38:644-650.
37. Silva BS, Yamamoto FP, Pontes FS, et al. TWIST and p-Akt immunoexpression in normal oral epithelium, oral dysplasia and in oral squamous cell carcinoma. *Med Oral Patol Oral Cir Bucal*. 2012;17:e29-34.
38. Segrelles C, Ruiz S, Perez P, et al. Functional roles of Akt signaling in mouse skin tumorigenesis. *Oncogene*. 2002;21:53-64.
39. Chen TC, Wu CT, Wang CP, et al. Significance of nuclear p-mTOR expression in advanced oral squamous cell carcinoma with extracapsular extension of lymph node metastases. Oral Oncol. 2015;51:493-499.
40. Nam SY, Lee HS, Jung GA, et al. Akt/PKB activation in gastric

carcinomas correlates with clinicopathologic variables and prognosis. *APMIS*. 2003;111:1105-1113.

41. Lim J, Kim JH, Paeng JY, et al. Prognostic value of activated Akt expression in oral squamous cell carcinoma. *J Clin Pathol*. 2005;58:1199-1205.
42. Hutchinson JN, Jin J, Cardiff RD, Woodgett JR, Muller WJ. Activation of Akt-1 (PKB-α) can accelerate ErbB-2-mediated mammary tumorigenesis but suppresses tumor invasion. *Cancer Res*. 2004;64:3171-3178.
43. Gulhati P, Bowen KA, Liu J, et al. mTORC1 and mTORC2 regulate EMT, motility, and metastasis of colorectal cancer via RhoA and Rac1 signaling pathways. *Cancer Res*. 2011;71:3246-3256.
44. Mikaelian I, Malek M, Gadet R, et al. Genetic and pharmacologic inhibition of mTORC1 promotes EMT by a TGF-β-independent mechanism. *Cancer Res*. 2013;73:6621-6631.

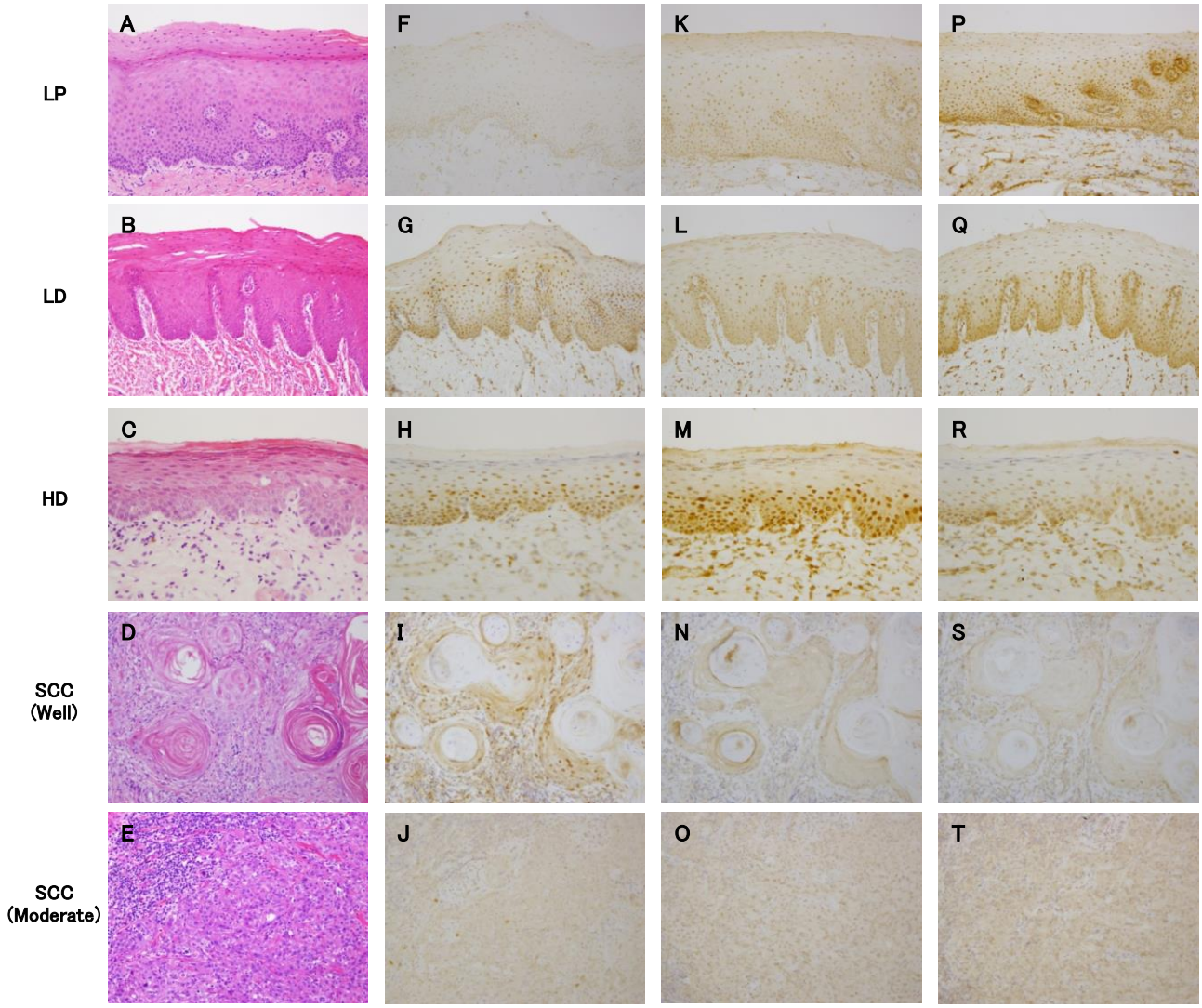

Fig. 3. Representative hematoxylin-eosin staining (**A–E**) and immunohistochemical staining for pAkt (**F–J**), pmTOR (**K–O**), and pSTAT3 (**P–T**) in leukoplakia (LP; **A**, **F**, **K**, **P**, ×200), low-grade epithelial dysplasia (LD; **B**, **G**, **L**, **Q**, ×200), high-grade epithelial dysplasia (HD; **C**, **H**, **M**, **R**, ×400), well-differentiated squamous cell carcinoma (SCC-Well; **D**, **I**, **N**, **S**, ×200), and moderately-differentiated squamous cell carcinoma (SCC-Moderate; **E**, **J**, **O**, **T**, ×200). pAkt showed weak cytoplasmic staining in epithelial cells (**F**). pAkt showed strong cytoplasmic and nuclear staining in the basal and prickle cell layers with colocalization of pmTOR and pSTAT3 expression (**G**, **H**, **L**, **M**, **Q**, **R**). pmTOR showed moderate cytoplasmic and nuclear staining in the basal and prickle cell layers (**K**). pSTAT3 showed strong cytoplasmic and nuclear staining in the basal and prickle cell layers (**P**). pAkt and pmTOR showed moderate or strong cytoplasmic and nuclear staining in most carcinoma cells, and pSTAT3 showed weak or moderate cytoplasmic and nuclear staining in most carcinoma cells (**I**, **J**, **N**, **O**, **S**, **T**).

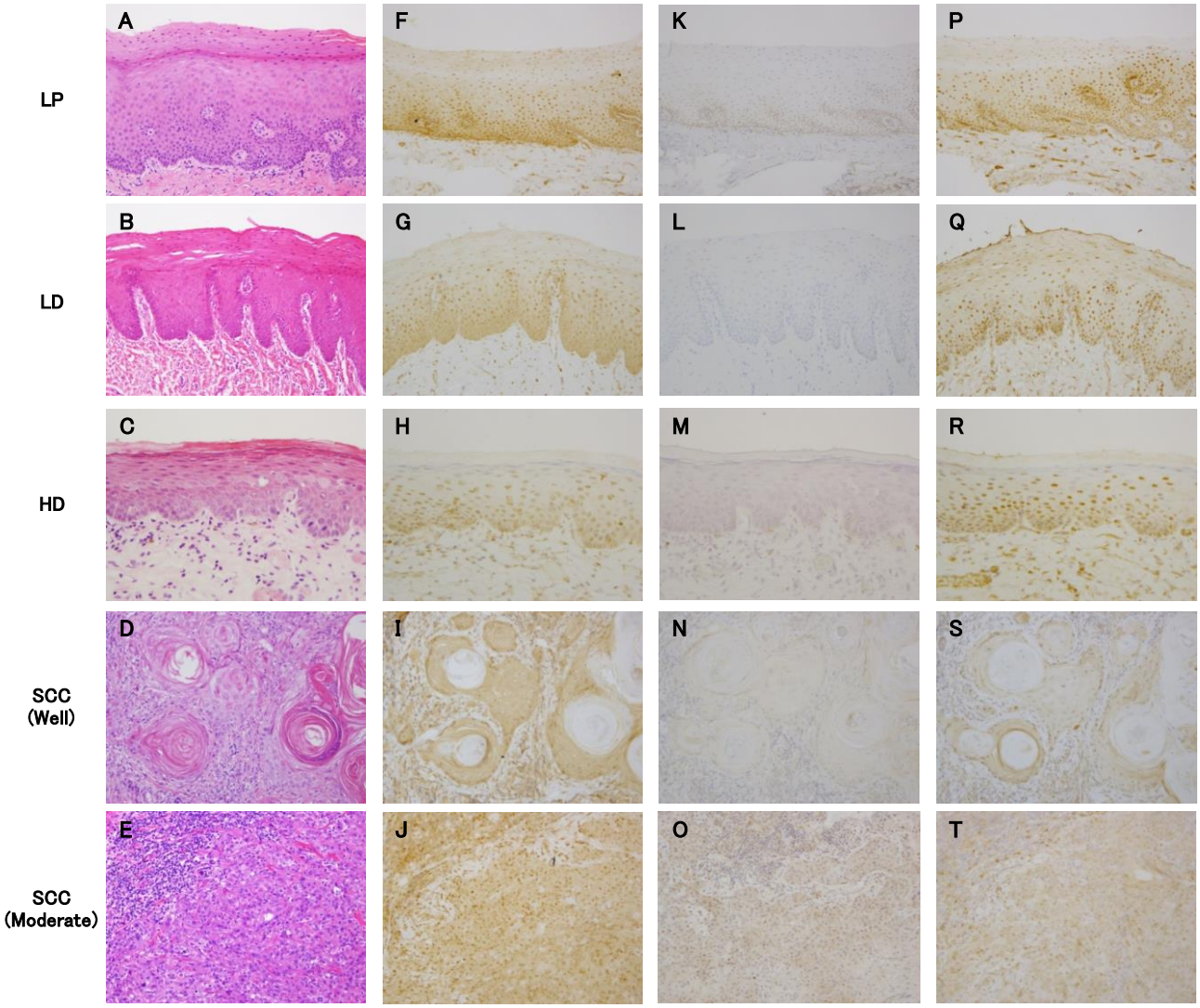

Fig. 2. Representative hematoxylin-eosin staining (**A–E**) and immunohistochemical staining for BRAF (**F–J**), BRAF-V600E (**K–O**), and pERK1/2 (**P–T**) in leukoplakia (LP; **A**, **F**, **K**, **P**, ×200), low-grade epithelial dysplasia (LD; **B**, **G**, **L**, **Q**, ×200), high-grade epithelial dysplasia (HD; **C**, **H**, **M**, **R**, ×400), well-differentiated squamous cell carcinoma (SCC-Well; **D**, **I**, **N**, **S**, ×200), and moderately-differentiated squamous cell carcinoma (SCC-Moderate; **E**, **J**, **O**, **T**, ×200). BRAF showed moderate or strong cytoplasmic staining in the basal and prickle cell layers and most carcinoma cells (**F–J**). BRAF-V600E showed negative expression (**K–M**). BRAF-V600E showed moderate or strong cytoplasmic staining in most carcinoma cells (**N**, **O**). pERK1/2 showed moderate or strong cytoplasmic and nuclear staining in the basal and prickle cell layers (**P**). pERK1/2 showed strong cytoplasmic and nuclear staining in the basal and prickle cell layers (**Q**, **R**). pERK1/2 showed moderate or strong cytoplasmic and nuclear staining in most carcinoma cells (**I**, **J**, **S**, **T**).

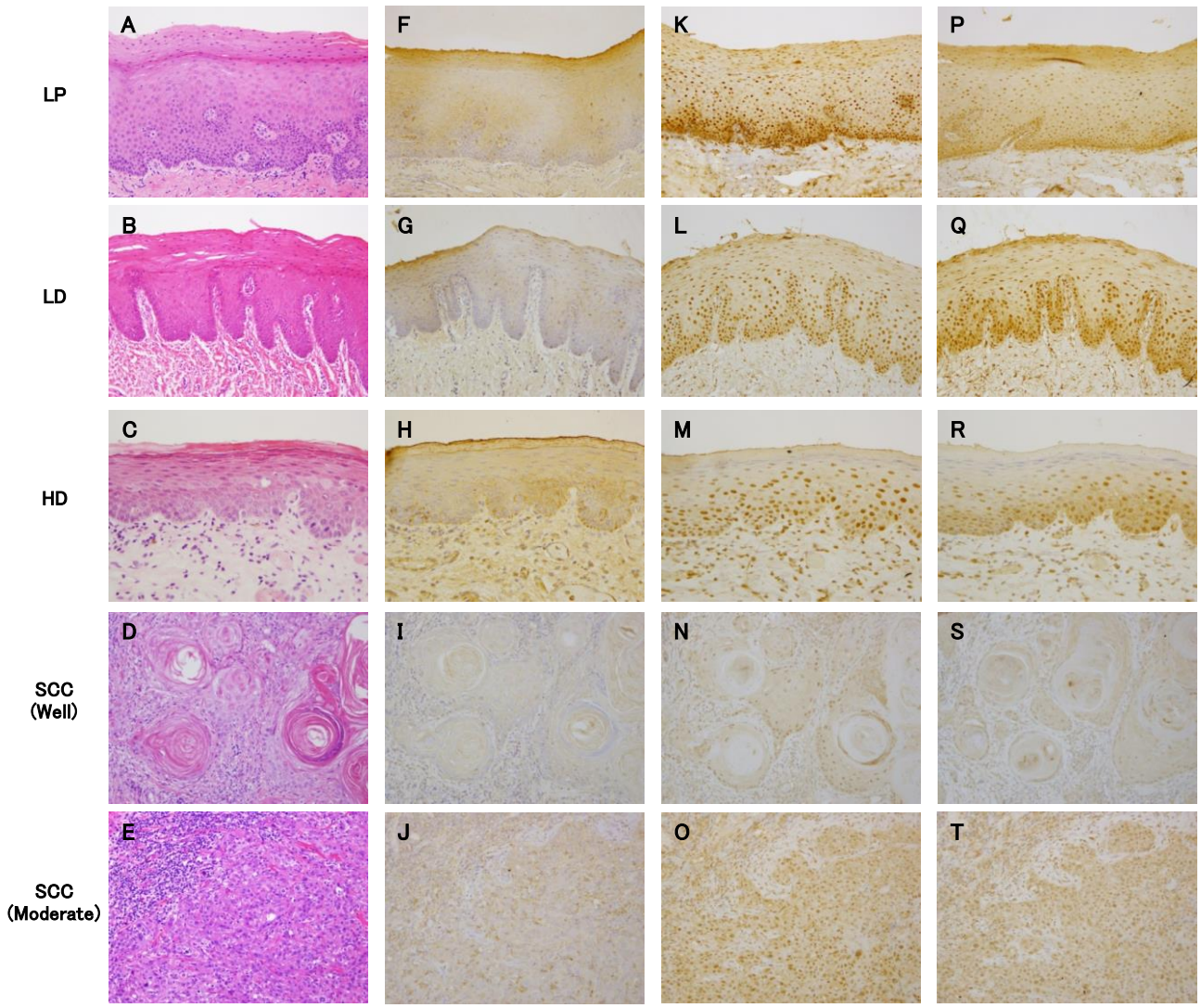

Fig. 1. Representative hematoxylin-eosin staining (**A–E**) and immunohistochemical staining for KRAS (**F–J**), HRAS (**K–O**), and NRAS (**P–T**) in leukoplakia (LP; **A**, **F**, **K**, **P**, ×200), low-grade epithelial dysplasia (LD; **B**, **G**, **L**, **Q**, ×200), high-grade epithelial dysplasia (HD; **C**, **H**, **M**, **R**, ×400), well-differentiated squamous cell carcinoma (SCC-Well; **D**, **I**, **N**, **S**, ×200), and moderately-differentiated squamous cell carcinoma (SCC-Moderate; **E**, **J**, **O**, **T**, ×200). KRAS showed moderate or strong cytoplasmic staining with occasional membrane reactivity in epithelial cells (**F–H**). KRAS showed weak or moderate cytoplasmic staining in most carcinoma cells (**I**, **J**). HRAS and NRAS showed moderate or strong cytoplasmic staining in the basal cell and parabasal cell layers (**K–M**, **P–R**). HRAS and NRAS showed moderate or strong cytoplasmic staining in most carcinoma cells (**N**, **O**, **S**, **T**).

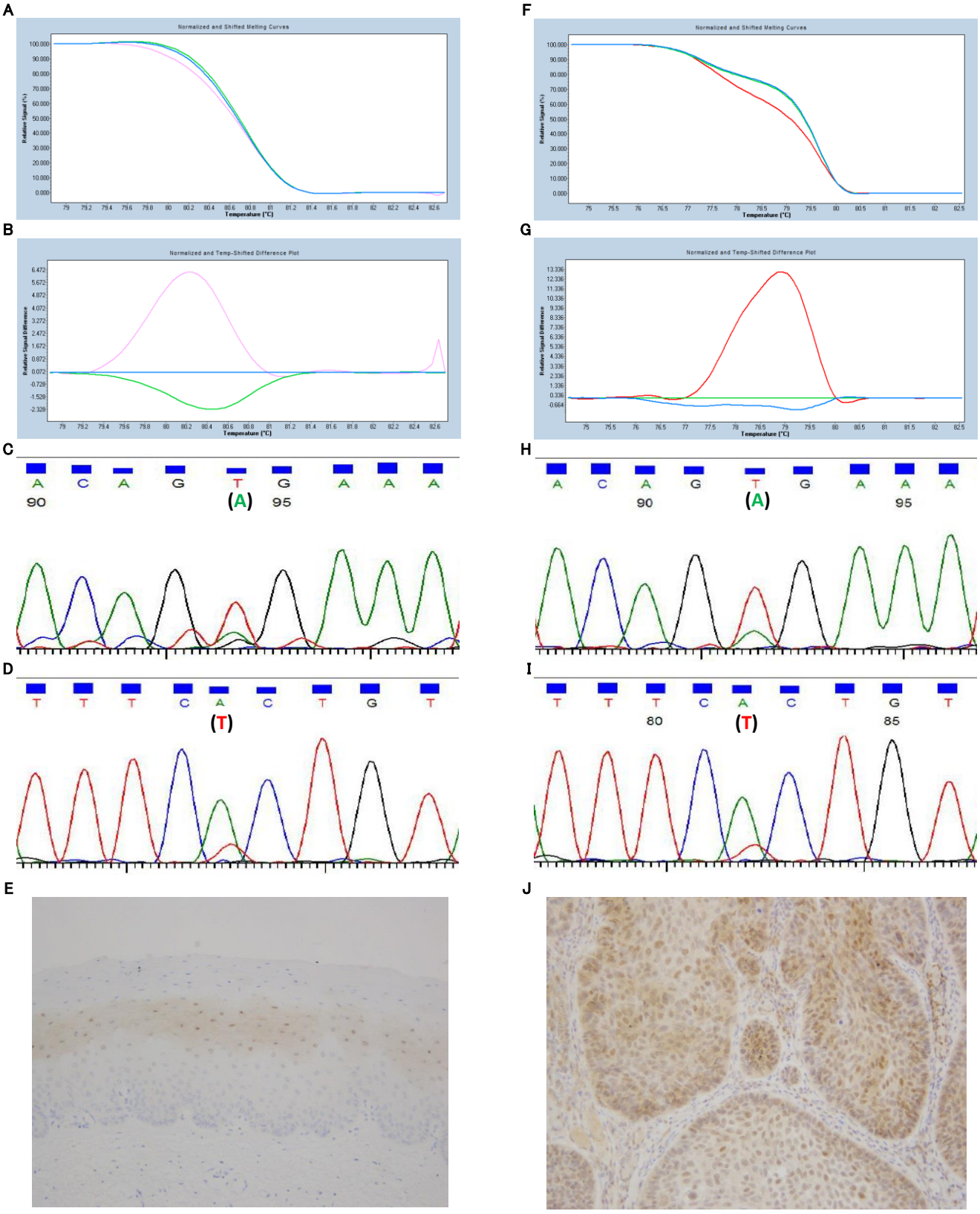

Fig. 4. Detection of *BRAF* mutations in patients with high-grade epithelial dysplasia (**A**–**E**) and well-differentiated squamous cell carcinoma (**F**–**J**) using high resolution melting (HRM) analysis, direct DNA sequence, and immunohistochemistry (IHC). The normalized high-resolution melting curves showed left-shifted curves in mutant samples (**A**, **F**). The temperature-shifted difference plots of each tested sample were subtracted from the reference curves obtained by analyzing control, wild type *BRAF* sequences (**B**, **G**). Sequencing results confirmed the presence of the *BRAF* mutations (T1799A) using forward (**C**, **H**) and reverse (**D**, **I**) primers. A BRAF-V600E IHC assay revealed weak expression in the prickle cell layer of an epithelial dysplasia specimen(**E**, ×200) and strong expression in most carcinoma cells from a squamous cell carcinoma specimen (**J**, ×200).

Table I. Immunohistochemical reactivity for KRAS, HRAS, NRAS, BRAF, BRAF-V600E, pERK1/2, pAkt, pmTOR, and pSTAT3 in oral epithelial precursor lesions and squamous cell carcinoma

	Number of cases	KRAS		HRAS		NRAS		BRAF		BRAF-V600E			pERK1/2		pAkt		pmTOR		pSTAT3	
	177	+	++	+	++	+	++	+	++	−	±	+	+	++	+	++	+	++	+	++
Leukoplakia without epithelial dysplasia（LP) (Squamous cell hyperplasia)	15	2 (13.3%)	13 (86.7%)	0 (0%)	15 (100%)	0 (0%)	15 (100%)	0 (0%)	15 (100%)	15 (100%)	0 (0%)	0 (0%)	5 (33.3%)	10 (66.7%)	10 (66.7%)	5 (33.3%)	8 (53.3%)	7 (46.7%)	0 (0%)	15 (100%)
Low-grade epithelial dysplasia (LD) (Mild to moderate epithelial dysplasia)	15	3 (20.0%)	12 (80.0%)	0 (0%)	15 (100%)	0 (0%)	15 (100%)	1 (6.7%)	14 (93.3%)	14 (93.3%)	1 (6.7%)	0 (0%)	2 (13.3%)	13 (86.7%)	4 (26.7%)	11 (73.3%)	0 (0%)	15 (100%)	0 (0%)	15 (100%)
High-grade epithelial dysplasia (HD) (Moderate to Severe epithelial dysplasia)	15	0 (0%)	15 (100%)	0 (0%)	15 (100%)	0 (0%)	15 (100%)	1 (6.7%)	14 (93.3%)	14 (93.3%)	1 (6.7%)	0 (0%)	0 (0%)	15 (100%)	7 (46.7%)	8 (53.3%)	0 (0%)	15 (100%)	0 (0%)	15 (100%)
Squamous cell carcinoma (SCC)	132	95 (72.0%)	37 (28.0%)	9 (6.8%)	123 (93.2%)	65 (49.2%)	67 (50.8%)	5 (3.8%)	127 (96.2%)	98 (74.2%)	29 (22.0%)	5 (3.8%)	16 (12.1%)	116 (87.9%)	33 (25.0%)	99 (75.0%)	9 (6.8%)	123 (93.2%)	16 (12.1%)	116 (87.9%)

Immunoreactivity except for BRAF-V600E
(+) : positive (reactive at the same level as adjacent normal part)
(++): strongly positive (strongly reactive as compared with adjacent normal part)

BRAF-V600E immunoreactivity
(−) : negative (no staining or only nuclear dot staining)
(±) : weak positive or ambiguous (immunostaining could not be evaluated as positive or negative)
(+) : positive (clear cytoplasmic staining)

Statistical significance
*$P < 0.05$
**$P < 0.01$
***$P < 0.001$

Table II. Correlation between clinical variables and immunoreactivity for KRAS, HRAS, NRAS, BRAF, BRAF-V600E, pERK1/2, pAkt, pmTOR, and pSTAT3 in oral squamous cell carcinoma

		Number of cases	KRAS			HRAS			NRAS			BRAF			BRAF-V600E				pERK1/2			pAkt			pmTOR			pSTAT3		
		132	+	++	*P value*	+	++	*P value*	+	++	*P value*	+	++	*P value*	−	±	+	*P value*	+	++	*P value*	+	++	*P value*	+	++	*P value*	+	++	*P value*
Age	20-29	2	2	0	<.001	1	1	.060	2	0	<.001	0	2	.590	1	1	0	.437	0	2	.292	1	1	.447	0	2	.184	0	2	.169
	30-39	3	3	0		0	3		2	1		0	3		2	1	0		0	3		0	3		0	3		0	3	
	40-49	15	14	1		1	14		6	9		0	15		10	5	0		0	15		6	9		0	15		0	15	
	50-59	17	11	6		2	15		15	2		2	15		13	3	1		0	17		3	14		1	16		2	15	
	60-69	30	26	4		1	29		21	9		2	28		27	2	1		5	25		8	22		2	28		8	22	
	70-79	39	34	5		2	37		19	20		1	38		28	9	2		8	31		11	28		1	38		5	34	
	80-89	24	5	19		1	23		0	24		0	24		15	8	1		3	21		3	21		5	19		1	23	
	90-99	2	0	2		1	1		0	2		0	2		2	0	0		0	2		1	1		0	2		0	2	
Sex	M	70	42	28	<.001	5	65	.060	23	47	<.001	1	69	.067	53	12	5	.440	12	58	.031	19	51	.275	6	64	.195	7	63	.216
	F	62	53	9		4	58		42	20		4	58		45	17	0		4	58		14	48		3	59		9	53	
Site	Tongue	71	43	28	.029	5	66	.237	24	47	.012	1	70	.139	49	20	2	.424	12	59	.122	17	54	.534	6	65	.514	7	64	.002
	Upper gingiva	11	11	0		0	11		8	3		2	9		8	2	1		1	10		1	10		0	11		2	9	
	Lower gingiva	24	18	6		1	23		18	6		2	22		18	4	2		0	24		5	19		1	23		2	22	
	Hard palate	2	1	1		0	2		1	1		0	2		2	0	0		0	2		1	1		0	2		2	0	
	Buccal mucosa	11	10	1		0	11		6	5		0	11		8	3	0		0	11		5	6		0	11		0	11	
	Floor of mouth	10	9	1		2	8		6	4		0	10		10	0	0		3	7		3	7		2	8		3	7	
	Lower lip	3	3	0		1	2		2	1		0	3		3	0	0		0	3		1	2		0	3		0	3	
T classification	1	40	27	13	.507	2	38	.842	15	25	.296	3	37	.357	28	8	4	.711	5	35	.012	9	31	.056	4	36	.689	6	34	.618
	2	41	33	8		4	37		24	17		1	40		30	10	1		10	31		16	25		3	38		6	35	
	3	17	11	6		1	16		9	8		1	16		13	4	0		1	16		4	13		1	16		2	15	
	4	34	24	10		2	32		17	17		0	34		27	7	0		0	34		4	30		1	33		2	32	
N classification	0	100	71	29	.899	7	93	.916	50	50	.582	4	96	.527	73	22	5	.309	16	84	.122	28	72	.279	8	92	.542	14	86	.596
	1	9	7	2		1	8		3	6		1	8		5	4	0		0	9		0	9		1	8		0	9	
	2	22	16	6		1	21		11	11		0	22		19	3	0		0	22		5	17		0	22		2	20	
	3	1	1	0		0	1		1	0		0	1		1	0	0		0	1		0	1		0	1		0	1	
M classification	0	126	89	37	.060	9	117	.254	61	65	.194	5	121	.316	92	29	5	.073	16	110	.179	30	96	.076	9	117	.254	16	110	.179
	1	6	6	0		0	6		4	2		0	6		6	0	0		0	6		3	3		0	6		0	6	
TNM Stage	Ⅰ	36	24	12	.297	2	34	.764	15	21	.570	3	33	.292	26	6	4	.537	5	31	.004	8	28	.097	4	32	.469	6	30	.432
	Ⅱ	38	31	7		4	34		22	16		1	37		28	9	1		10	28		15	23		2	36		6	32	
	Ⅲ	20	12	8		1	19		10	10		1	19		13	7	0		1	19		4	16		2	18		1	19	
	Ⅳ	38	28	10		2	36		18	20		0	38		31	7	0		0	38		6	32		1	37		3	35	
Recurrence	Negative	113	83	30	.180	9	104	.103	58	55	.123	5	108	.178	83	26	4	.331	15	98	.163	30	83	.160	9	104	.103	16	97	.041
	Positive	19	12	7		0	19		7	12		0	19		15	3	1		1	18		3	16		0	19		0	19	
Postoperative metastasis (regional lymph node)	Negative	116	82	34	.191	8	108	.465	58	58	.322	5	111	.199	89	24	3	.030	15	101	.224	26	90	.033	8	108	.465	13	103	.196
	Positive	16	13	3		1	15		7	9		0	16		9	5	2		1	15		7	9		1	15		3	13	
Survival	Alive	108	78	30	.450	7	101	.424	55	53	.130	3	105	.288	80	23	5	.297	13	95	.195	26	82	.419	9	99	.098	15	93	.150
	Dead	19	14	5		1	18		7	12		1	18		15	4	0		1	18		5	14		0	19		1	18	
	Dead of other disease	2	1	1		1	1		1	1		0	2		0	2	0		1	1		1	1		0	2		0	2	
	Unknown	3	2	1		0	3		2	1		1	2		3	0	0		1	2		1	2		0	3		0	3	

Immunoreactivity except for BRAF-V600E

(−) : negative

(+) : positive (reactive at the same level as adjacent normal part)

(++) : strongly positive (strongly reactive as compared with adjacent normal part)

BRAF-V600E immunoreactivity

(−) : negative (no staining or only nuclear dot staining)

(±) : weak positive or ambiguous (immunostaining could not be evaluated as positive or negative)

(+) : positive (clear cytoplasmic staining)

Statistical significance

*P < 0.05

**P < 0.01

***P < 0.001

Table III. Correlation between pathological variables and immunoreactivity for KRAS, HRAS, NRAS, BRAF, BRAF-V600E, pERK1/2, pAkt, pmTOR, and pSTAT3 in oral squamous cell carcinoma

		Number of cases	KRAS			HRAS			NRAS			BRAF			BRAF-V600E				pERK1/2			pAkt			pmTOR			pSTAT3		
		132	+	++	*P value*	+	++	*P value*	+	++	*P value*	+	++	*P value*	−	±	+	*P value*	+	++	*P value*	+	++	*P value*	+	++	*P value*	+	++	*P value*
Degree of defferentiation	Well	110	77	33	.503	7	103	.342	54	56	.997	5	105	.597	80	28	2	.767	16	94	.164	26	84	.195	8	102	.182	16	94	.164
	Moderate	18	15	3		1	17		9	9		0	18		15	1	2		0	18		7	11		0	18		0	18	
	Poor	4	3	1		1	3		2	2		0	4		3	0	1		0	4		0	4		1	3		0	4	
Stromal lymphocytic reaction	Slight	12	9	3	.767	2	10	.349	6	6	.998	1	11	.669	8	4	0	.663	2	10	.774	5	7	.283	1	11	.910	2	10	.219
	Moderate	118	85	33		7	111		58	60		4	114		89	24	5		14	104		28	90		8	110		13	105	
	Severe	2	1	1		0	2		1	1		0	2		1	1	0		0	2		0	2		0	2		1	1	
Mode of invasion	2	17	14	3	.112	1	16	.377	10	7	.091	1	16	.927	12	5	0	.483	2	15	.605	4	13	.520	0	17	.020	3	14	.582
	3	85	60	25		8	77		43	42		3	82		65	17	3		12	73		22	63		7	78		9	76	
	4C	24	19	5		0	24		12	12		1	23		18	5	1		1	23		7	17		0	24		4	20	
	4D	6	2	4		0	6		0	6		0	6		3	2	1		1	5		0	6		2	4		0	6	
Invasion depth	Microinvasion	36	27	9	.785	4	32	.426	20	16	.335	2	34	.737	26	9	1	.282	7	29	.064	13	23	.195	2	34	.358	9	27	.021
	Mucosal tissue	51	35	16		2	49		21	30		2	49		42	6	3		2	49		11	40		2	49		4	47	
	Submucosal tissue	45	33	12		3	42		24	21		1	44		30	14	1		7	38		9	36		5	40		3	42	

Immunoreactivity except for BRAF-V600E

(–) : negative

(+) : positive (reactive at the same level as adjacent normal part)

(++) : strongly positive (strongly reactive as compared with adjacent normal part)

BRAF-V600E immunoreactivity

(–) : negative (no staining or only nuclear dot staining)

(±) : weak positive or ambiguous (immunostaining could not be evaluated as positive or negative)

(+) : positive (clear cytoplasmic staining)

Statistical significance

*$P < 0.05$

Table IV. Correlation of detected *BRAF* mutations among IHC, HRM, direct DNA sequencing, and in oral epithelial precursor lesions and squamous cell carcinoma

	IHC					HRM				Sequence			
	Total	–	±	+	*P value*	Total	Wild	Mutant or ambiguous	*P value*	Total	Wild	Mutant	*P value*
Leukoplakia without epithelial dysplasia（LP) (Squamous cell hyperplasia)	15	15	0	0	.093	15	11	4	.297	4	4	0	.067
Low-grade epithelial dysplasia (LD) (Mild to moderate epithelial dysplasia)	15	14	1	0		15	13	2		2	1	1	
High-grade epithelial dysplasia (HD) (Moderate to Severe epithelial dysplasia)	15	14	1	0		15	14	1		1	0	1	
Squamous cell carcinoma (SCC)	132	98	29	5		132	98	34		34	29	5	

IHC, Immunohistochemistry; HRM, High resolution melting

Table V. Correlation of detected *BRAF* mutations between IHC and direct DNA sequencing in oral epithelial precursor lesions and squamous cell carcinoma

		Sequence							
		OEPLs				SCC			
		Wild	Mutant	Total	*P value*	Wild	Mutant	Total	*P value*
IHC	–	5	0	5	.014	11	0	11	<.001
	±	0	2	2		18	0	18	
	+	0	0	0		0	5	5	
Total		5	2	7		29	5	34	

IHC, Immunohistochemistry; OEPLs, Oral epithelial precursor lesions

Statistical significance
*$P < 0.05$
***$P < 0.001$

Table VI. List of cases of detected *BRAF* mutations by both molecular assays and IHC

Case	Age (Year)	Sex	Site	TNM classification	TNM Stage	Recurrence	Postoperative metastasis (regional lymph node)	Survival	Degree of defferentiation	Stromal lymphocytic reaction	Mode of invasion	Invasion depth
LD	79	M	Upper gingiva									
HD	61	F	Tongue									
SCC	57	M	Tongue	T1N0M0	Ⅰ	Yes	Yes	Alive	Moderate	Moderate	4C	Submucosal tissue
SCC	60	M	Lower gingiva	T2N0M0	Ⅱ	No	Yes	Alive	Low	Moderate	4D	Mucosal tissue
SCC	70	M	Tongue	T1N0M0	Ⅰ	No	No	Alive	Well	Moderate	3	Mucosal tissue
SCC	77	M	Lower gingiva	T1N0M0	Ⅰ	Yes	No	Alive	Well	Moderate	3	Microinvasion
SCC	81	M	Upper gingiva	T1N0M0	Ⅰ	No	No	Alive	Moderate	Moderate	3	Mucosal tissue

IHC, Immunohistochemistry; LD, Low-grade epithelial dysplasia (Mild to moderate epithelial dysplasia); HD, High-grade epithelial dysplasia (Moderate to Severe epithelial dysplasia); SCC, Squamous cell carcinoma.